J Comput Electron (2007) 6:219–222
DOI 10.1007/s10825-006-0105-7

Simulation of high-field magnetotransport in non-planar 2D electron systems

Gregory J. Meyer · Irena Knezevic

Published online: 18 January 2007

Abstract We present a simulation of ballistic magnetotransport in a curved resonant quantum cavity, a non-planar two-dimensional (2D) electron system formed by partial release of the planar cavity under strain. A transfer-matrix technique originally due to Usuki and coworkers [Phys. Rev. B 52, 8244 (1995)] has been adapted to ensure the technique's continued dependability at high magnetic fields, and accommodate the nonzero local curvature of the simulated system. Conductance in non-planar structures is found to be highly sensitive to the changes in the curvature, indicating their potential in NEMS and sensing applications.

Keywords Magnetotransport · Transfer matrix · curved geometries · Peierls substitution

1 Introduction

Non-planar two-dimensional (NP2D) electron systems have started to attract enhanced theoretical attention [1, 2], as they are now being fabricated in a variety of configurations, on both III-V thin film heterostructures [3–5] and strained Si/SeGe nanomembranes [6–8]. Curvature becomes another degree of freedom available for manipulating electronic properties of these systems, which leads to novel basic physics and suggests NP2D application in NEMS as ultrasensitive scales and sensors.

G. J. Meyer (✉) · I. Knezevic
Department of Electrical and Computer Engineering, University of Wisconsin-Madison, 1415 Engineering Dr, Madison, WI 53706, USA
e-mail: gjmeyer@wisc.edu

I. Knezevic
e-mail: knezevic@engr.wisc.edu

In this paper, we report calculations of high-field magnetotransport in a ballistic curved resonant quantum cavity (RQC). This NP2D electron system is formed at the junction of a GaAs/InGaAs heterostructure by creating two symmetric constrictions (of 50 nm width) in a 300 nm wide quantum wire (Fig. 1). Upon selective underetching of the sacrificial layer, strain relaxation causes the wings of the cavity to roll into a partial cylinder, while the central spine remains tethered to the substrate [7]. (This design loosely follows that of Ref. [9], however those experiments dealt with pronouncedly scattering-limited transport at non-cryogenic temperatures.) Planar RQCs of similar construction have been studied extensively and their transport properties are well-known [13]. Cylindrical structures, however, display interesting physics on a number of levels. Their curvature induces an attractive geometric potential [10], inversely proportional to the radius of curvature squared. Moreover, their surfaces do not remain normal to the direction of the magnetic field, creating non-uniformities in the flux. However, computationally efficient modeling of quantum-scale transport under strong magnetic fields (>1 T) has been a challenge. Therefore, we have adapted a variant of the transfer-matrix method [11–13] to incorporate non-planar (specifically cylindrical) geometries and high magnetic fields. The transfer-matrix method is an efficient, flexible, and widely-used tool for modeling ballistic quantum transport in planar 2D electron systems at low bias. Magnetotransport calculations can be performed efficiently within the approach of Refs. [11, 12] at low magnetic fields through the use of the Peierls substitution [14]. We have made two modifications to this method in order to address its two current limitations: we re-derived the Peierls phase in order to address non-planar geometries, and have altered the mode selection procedure in order to stabilize the method for high magnetic fields.

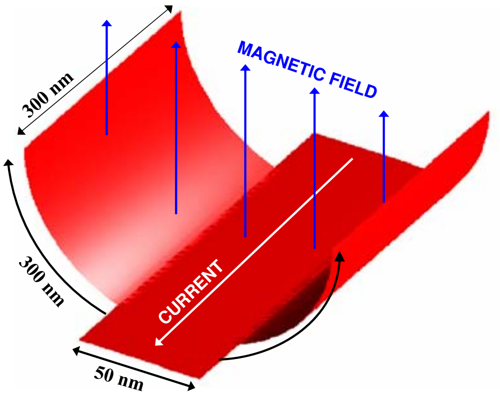

Fig. 1 The cylindrical quantum cavity in a uniform magnetic field

2 Transfer-matrix method in high magnetic fields

The transfer-matrix method is an iterative routine derived from the discretized Schrödinger equation. The Peierls substitution [14] provides a gauge-invariant way to incorporate the magnetic field into this equation. Namely, upon discretizing the zero-field Schrödinger equation in a general form

$$t_{mn}\psi_n = E\psi_m, \tag{1}$$

the magnetic field can be introduced by replacing

$$t_{mn} \to t_{mn} \exp\left(\frac{ie}{\hbar}\int_n^m \vec{A}\cdot d\vec{l}\right), \tag{2}$$

where the above integral of the magnetic vector potential must be taken *along the straight line* connecting the n-th and m-th meshpoint on the grid. This substitution has the effect of producing the $(\vec{p}+e\vec{A})^2$ term in the magnetic field, as it performs the extra magnetic field translation due to $\vec{A}$. More information on the Peierls substitution in periodic lattices (real or numerical) can be found in Refs. [15–17].

The discretized Schrödinger equation can be arranged into an iterative procedure to solve for the electron wavefunction slice by slice along the direction of current flow (t is the nearest-neighbor hopping energy):

$$\begin{bmatrix}\psi_l\\ \psi_{l+1}\end{bmatrix} = \underbrace{\begin{bmatrix}\hat{0} & \hat{I}\\ -\hat{H}_{l,l+1}^{-1}\hat{H}_{l,l-1} & \hat{H}_{l,l+1}^{-1}(E\hat{I}-\hat{H}_l)\end{bmatrix}}_{\hat{T}_l}\begin{bmatrix}\psi_{l-1}\\ \psi_l\end{bmatrix}, \tag{3a}$$

$$\hat{H}_{l,l+1} = diag\left[-t\exp\left(\frac{ieBa^2}{2\hbar}\right)\dots - t\exp\left(\frac{ieBa^2M}{2\hbar}\right)\right], \tag{3b}$$

$$\hat{H}_{l,l-1} = \hat{H}_{l,l+1}^{\dagger} \tag{3c}$$

Here, M is the dimension of the grid in the direction perpendicular to the current flow.

In order to calculate conductance across a 2D structure, the transmission coefficient must be obtained for each current-carrying mode. Modes are injected as plane waves in the left contact, through $\psi_1 = \psi_0\exp(ika)$, and solution to Eq. (3a) with $l = 0$ gives $2M$ modes. Since modes propagating in the assumed direction of current flow are the only ones that contribute to the conductance, they must be selected from the large number of $\exp(ika)$ eigenvalues of the matrix $\hat{T}_0$. In the absence of a magnetic field this is a straightforward process: propagating modes will have real k values, and $|\exp(ika)| = 1$, and forward modes will have positive k values, and $\sin(ka) > 0$. Note that the grid spacing a must be sufficiently small to ensure that all $ka < \pi$.

In zero magnetic field, exactly M of the $2M$ modes are forward modes and M are backward modes, where each direction contains both propagating and evanescent modes. This symmetry stems from the real matrix elements of the $2M \times 2M$ matrix $\hat{T}_0$ defined in Eq. (3a). However, with the application of the magnetic field, the matrix ceases being real, and there is no more guarantee that forward and backward propagating modes will occur in pairs. Unfortunately, this requirement is necessary to maintain the Usuki iteration procedure stability.

As the magnetic field strength is increased, the eigenvalues are commingled with the Peierls phase, and it becomes difficult to distinguish forward from backward modes. The problem can be reduced greatly with a simple shift of coordinates within the simulated ℓ-th slice: moving the origin to the slice center, thereby counting the meshpoints within the slice as going from $-M/2$ to $M/2$. Placing the origin in the center of the domain yields a symmetric shift that does not artificially advance the eigenvalue's phase. The selection rules will correctly identify forward propagating modes over a much wider range of field strengths (see Fig. 2) and thus yield stable and accurate conductance results.

3 Peierls phase in non-planar geometries

For non-planar geometries, $\int \vec{A}\cdot d\vec{\ell}$ that corrects the zero-field matrix elements t_{mn} must be taken over a geodesic between n and m. As an example, we model a quantum cavity whose wings have been allowed to curl, but whose center is held flat by thin metallic contacts (see Fig. 1).

$\int \vec{A}\cdot d\vec{\ell}$ taken along a geodesic on the surface of a cylinder, in parameterized coordinates x and s, yields

$$\int \vec{A}\cdot d\ell = \frac{x_2-x_1}{s_2-s_1}BR^2\left[\cos\frac{s_2}{R} - \cos\frac{s_1}{R}\right] \tag{4}$$

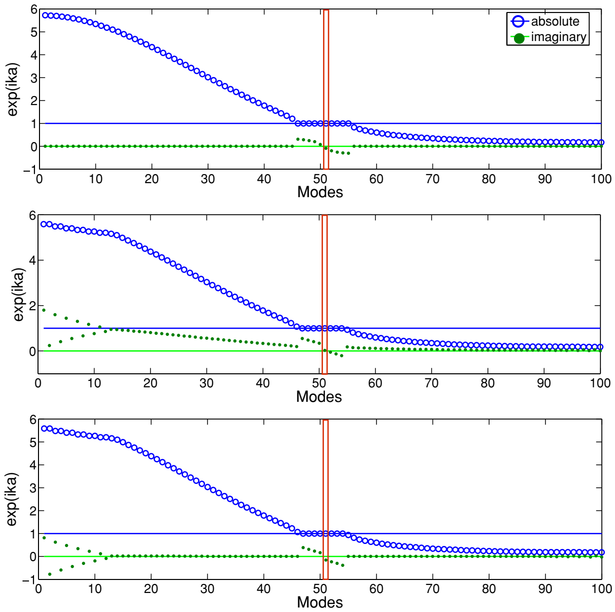

Fig. 2 Absolute values and imaginary components of all modes for a 300 nm wire at $N = 10^{11}$ cm^{-2} and B = 0 (top graph) and B = 0.6 Tesla (lower graphs). Applying Peierls phase skews the imaginary values of all eigenvalues and erroneously reports an extra forward propagating mode under this moderate magnetic field (middle graph). This skewing effect is minimized by taking $\int \vec{A} \cdot d\vec{\ell}$ from the center of each slice rather than the edge (bottom graph)

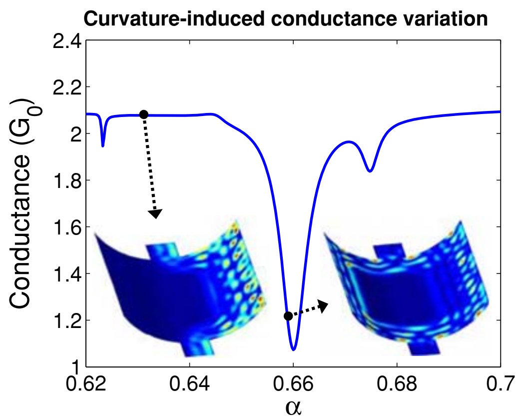

Fig. 3 At a magnetic field of 3 Tesla and a Fermi energy of 3.7 meV, conductance through the cavity varies on account of the cyclotron orbits alternately being closed (the electron hops over the contact), and open (the electron exits into the drain). The curvature, measured by the parameter α equal to the ratio of the wire width and the radius of curvature (in the units of π), is the source of this edge state variation

where R is the constant radius of curvature of the cylindrical portion of the cavity. For the flat portion of our structure, R goes to infinity, and Eq. (4) reverts to its planar form.

4 Results

The modified transfer-matrix method produces results that confirm what is known about the physics of high-field magnetotransport in planar structures, such as edge states and depopulation of Landau levels. In curved structures, it illuminates some novel features, such as dependence of the conductance on the curvature at a given magnetic field.

For example, at select magnetic fields, the conductance is very sensitive to increasing curvature: as shown in Fig. 3 for 2.5 T, conductance in the flat cavity is small, owing to the closed orbits and the carrier hopping over instead of into the drain. Even a relatively small increase in curvature disturbs the closed orbits and shuttles the electron into the drain. Also, curvature disturbs (broadens and shifts) initially well-defined edge states, as seen in Fig. 4. These phenomena provide a mechanism to manipulate the conductance of the cavity through curvature, making it a good candidate for certain types of sensors.

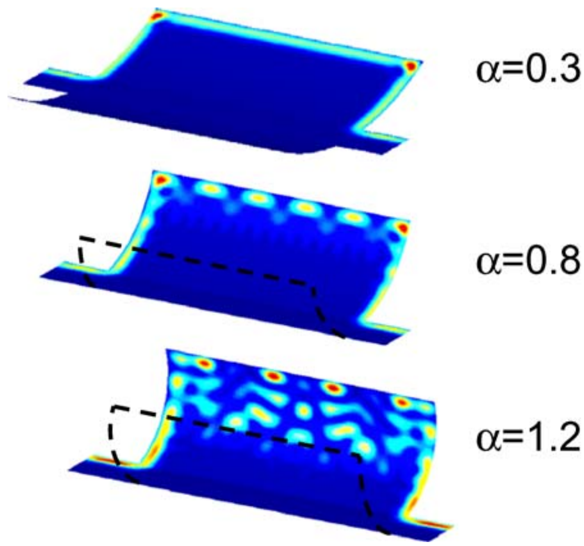

Fig. 4 Curvature broadens and shifts edge state. The near wing of the cavity has been removed in the lower two images to provide a better view of the edge state evolution; probability in the near wing is effectively 0. Magnetic field is 8 Tesla, Fermi energy is again 3.7 meV

5 Conclusion

The transfer matrix method has long been an effective way to calculate quantum transport in low-field, planar 2D electron systems. With the modifications put forth in this paper, it is now equally effective in high field and non-planar conditions. We presented a comprehensive magnetotransport calculation on a cylindrical resonant quantum cavity, a non-planar 2D electron system, and showed the dependence of its conductance on the curvature. The interplay of electronics and geometry that characterized these novel nanostructures reveals their large potential in NEMS and sensing applications.

Acknowledgment This work is funded by the NSF through the UW MRSEC. We would like to acknowledge Prof. Robert Blick for bringing these curved heterostructures to our attention.

References

1. Chaplik, A.V., et al.: Ballistic transport in quantum cylinders. Superlatt. Microstruct. **23**, 1227 (1998)
2. Marchi, A., Reggiani, S., Rudan, M., Bertoni, A.: Coherent electron transport in bent cylindrical surfaces. Phys. Rev. B **72**, 035403 (2005)
3. Prinz, Y.Ya., Seleznev, V.A., Gutakovsky, A.K., Chehovskiy, A.V., Preobrazhenskii, V.V., Putyato, M.A., Gavrilova, T.A.: Free-standing and overgrown InGaAs/GaAs nanotubes, nanohelices and their arrays. Physica E **6**, 828–831 (2000)
4. Mendach, S., Kipp, T., Welsch, H., Heyn, Ch., Hansen, W.: Interlocking mechanism for the fabrication of closed single-walled semiconductor microtubes. Semicond. Sci. Technol. **20** 402–405 (2005)
5. Lorke, A., et al.: Curved two-dimensional electron gases. Superlatt. Microstruct. **33**, 347 (2003)
6. Golod, S.V., Prinz, V.Ya., Mashanov, V.I., Gutakovsy, A.K.: Fabrication of conducting GeSi/Si micro- and nanotubes and helical microcoils. Semicond. Sci. Technol. **16**, 181–185 (2001)
7. Roberts, M.M., Klein, L.J., Savage, D.E., Friesen, M., Celler, G.K., Eriksson, M.A., Lagally, M.G.: Elastically relaxed free-standing strained-silicon nanomembranes. Nat. Mater. **5**, 388–393 (2006)
8. Qin, H., Shaji, N., Merrill, N.E., Kim, H.S., Toonen, R.C., Blick, R.H., Roberts, M.M., Savage, D.E., Lagally, M.G., Celler, G.: Formation of micro-tubes from strained SiGe/Si heterostructures. New J. Phys. **7**, 241 (2005)
9. Shaji, N., et al.: submitted
10. DaCosta, R.T.: Quantum mechanics of a constrained particle. Phys. Rev. A **34**, 1982 (1981)
11. Ando, T.: Quantum point contacts in magnetic fields. Phys. Rev. B **44**(15), 583–632 (1991)
12. Usuki, T., Saito, M., Takatsu, M., Kiehl, R.A., Yokoyama, N.: Numerical analysis of ballistic-electron transport in magnetic fields by using a quantum point contact and a quantum wire. Phys. Rev. B **52**(11), 8244–8255 (1995)
13. Bird, J.P., Akis, R., Ferry, D.K., deMoura, A.P.S., Lai, Y.-C., Indlekofer, K.M.: Interference and interactions in open quantum dots. Rept. Prog. Phys. **66**, 8017–8027 (2003)
14. Peierls, R.E.: On the theory of the diamagnetism of conduction electrons. Zeitschrift für Physik **80**, 763–791 (1933)
15. Hofstadter, D.R.: Energy levels and wave functions of Bloch electrons in rational and irrational magnetic fields. Phys. Rev. B **14**, 2239 (1976)
16. Luttinger, J.M.: The effect of a magnetic field on electrons in a periodic potential. Phys. Rev. **84**, 814 (1951)
17. Kohn, W.: Analytical properties of bloch waves and wannier functions. Phys. Rev. **115**, 1460 (1959)